

Γ phonons and microscopic structure of orthorhombic KNbO_3 from first-principles calculations

A. V. Postnikov,* and G. Borstel

Universität Osnabrück – Fachbereich Physik, D-49069 Osnabrück, Germany

(January 1, 2018)

From a series of total energy calculations by the full-potential linear muffin-tin orbital method, the total energy hypersurface as function of atomic displacements from equilibrium positions has been fitted for different Γ phonon modes in orthorhombic KNbO_3 . Frequencies and eigenvectors of all TO Γ phonons have been calculated in the harmonic approximation, and in the quantum oscillator scheme – for A_2 and B_2 modes. The microscopic structure of the orthorhombic phase has been analyzed in a series of supercell calculations for different patterns of Nb displacements, providing indications in favour of the chain structure, with oppositely directed neighboring chains.

63.20.-e, 63.75.+z, 71.10.+x, 77.80.Bh

I. INTRODUCTION

Of three ferroelectric phases known for potassium niobate, the orthorhombic phase is probably the best experimentally studied. This is a room-temperature phase which exists in the temperature range -10 to 225 °C and is therefore the most important for any practical applications, e.g., related to the photorefractive properties of KNbO_3 . Considerable amount of information has been accumulated from Raman scattering [1,2,3] and neutron scattering [4] experiments; local environment of Nb atoms has been probed by EXAFS measurements [5]; recent experiments on impulsive simulated (time-resolved) Raman scattering [6,7] provide additional data on oscillatory and relaxation-type phonon modes. However, the understanding, on the theoretical level, of fine mechanisms behind ferroelectric atomic displacements and phase transitions in KNbO_3 is still not sufficient. *Ab initio* calculations which may clarify this point have not been up to now performed, to our best knowledge, for the orthorhombic phase, because of the lower symmetry and correspondingly higher calculational effort demanded, as compared to the cubic (non-polar) phase and the tetragonal ferroelectric phase.

In the present paper, we extend our previous research on the equilibrium geometry of the ferroelectric ground state structure of KNbO_3 [8] and on phonon properties in cubic and tetragonal phases [9] onto the orthorhombic phase of this material. The band structure and total energy calculations, based on which the equilibrium geometry and phonon properties are investigated, have been performed using the full-potential linear muffin-tin orbital code by Methfessel [10,11]. The technical aspects of the calculations for KNbO_3 are discussed in some detail in Ref. [8].

Apart from lower symmetry, another difficulty in performing the calculations for the orthorhombic phase is the much smaller magnitude of relevant energy differences, e.g., related to the displacements within the soft mode, as compared to cubic or tetragonal phases. This demands an accuracy of total energy calculation of at least 0.01 mRy. In the computer code we applied, that is technically possible due to the use of the Harris energy which coincides with the Kohn–Sham energy in the first order with respect to variations around the self-consistent density and converges much more smoothly than the latter. (More details on the properties of the Harris functional and its applications may be found in Ref. [12]). Also, the convergence of the total energy in the number of special points in the Brillouin zone has to be particularly strictly controlled. The corresponding error was always within 0.01 mRy in our calculations even for different supercell geometries (with different patterns of the \mathbf{k} -points for integration) if they actually refer to the same crystal (super)structure [13].

The paper is organized as follows: In section II, the geometry optimization in the orthorhombic phase is discussed and compared with the experimental data. In section III, the results of the frozen phonon calculations in the harmonic approximation are presented, and in section IV – the analysis of phonon frequencies in terms of the quantum oscillator model. Finally, in section V different models for the microscopic structure of the orthorhombic phase are considered, and the relevance of the chain structures is emphasized.

II. OPTIMIZED STRUCTURE OF THE ORTHORHOMBIC PHASE

In discussing the geometry of the orthorhombic phase, we follow the notations introduced by Hewat [14]: three lattice vectors are $a=3.973$ Å along $\mathbf{x} = [100]$ of the cubic aristotype; $b=5.695$ Å along $\mathbf{y} = [0\bar{1}1]$ and $c=5.721$ Å

along $\mathbf{z} = [011]$. The positions of atoms and the magnitudes of their off-center displacements in terms of these lattice vectors are given in Table I. It would be in principle possible in a first-principle calculation to minimize the total energy with respect to all seven independent structure parameters, i.e., three lattice vectors and four internal atomic displacements. The optimization of such multidimensional function is however computationally very demanding and hardly likely to produce any new essential information. Based on our previous experience, gained from the study of tetragonal KNbO_3 , that the lattice strain found from the total energy minimization is in very good agreement with experiment [8], and in order to keep the number of independent parameters in the structure optimization manageable, we fixed the lattice volume and strain in our frozen phonon calculations and used for the lattice parameters the experimental data of Ref. [14]. However, all off-center displacements of atoms, which are allowed by symmetry, have to be optimized in the calculation, in order to guarantee that for each phonon, the force constants are calculated near the total energy minimum. The optimization has been performed by the polynomial fit of the total energy as function of four variables; the values of parameters corresponding to the total energy minimum are also given in Table I. Similarly to the choice of Ref. [14], we kept Nb in the center of the cube and allowed all other atoms to relax with respect to it. Comparing the calculated and experimental values of Δ 's in Table I, one can conclude that the z -displacement of oxygen atoms is fairly well reproduced, including the fact that O_1 is slightly farther shifted than O_2, O_3 . The y -displacement of O_2 is larger than the experimental estimate; it should be noted however that the magnitude of this displacement is very small, and of primary importance is the fact that the calculation correctly reproduces the sign of this parameter. Finally, the z -displacement of K is overestimated by almost a factor of 3, that is identical to what we have found earlier when optimizing the geometry of the tetragonal phase [9]. In other words, in our calculations K tends to remain coupled to the oxygen sublattice, so that the ferroelectric distortion arises roughly due to the pure displacement of Nb.

III. FROZEN PHONONS

Combined atomic displacements in the orthorhombic phase which has the space group $Amm2$ (No. 38 of the International tables) are split by symmetry into four one-dimensional irreducible representations. After projecting out three translational modes similarly to how it was discussed in some detail by Cohen and Krakauer for cubic BaTiO_3 [15], one stays with 12 symmetry coordinates S_t . The choice of S_t (arbitrary up to constructing other linear combinations within each irreducible representation) we used in our total energy fitting and frozen phonon calculations, in terms of cartesian displacements of atoms 1 to 5 according to Table I, is given in Table II.

We calculated the total energy within each irreducible representation for a sufficient number of different displacement patterns as to make a fit by the fourth-order polynomial. Apart from extracting second derivatives for the force constants, this fit made possible the quantum oscillator analysis described below in section IV and the optimization of finite displacements within the soft mode. A list of polynomial coefficients for the B_2 representation, that is probably of the most general interest since it contains the soft mode, is given in Table III. Total energy in mRy may be restored as the sum over all coefficients multiplied by corresponding powers of S_t in a.u.

In constructing the kinetic-energy matrix and solving the eigenvalue problem for the TO Γ phonons in the harmonic approximation, we followed the guidelines of Ref. [16] (see also Ref. [15] for some details). Calculated frequencies are given in Table IV along with the eigenvectors, which are expressed in terms of cartesian displacements of individual atoms (relative to the center of mass), multiplied by the square roots of masses, via back transformation from the symmetry coordinates defined in Table II. The comparison with experimentally measured frequencies is given in Table V. The overall agreement with experiment is within about 10%, with the exception of $\text{TO}_2 B_1$ mode and the A_2 mode. For the B_1 phonon, the difference is probably due to some inaccuracy in the polynomial fit to the four-dimensional total energy hypersurface, since the frequency of the corresponding vibration (K – Nb stretching on the background of relatively undistorted oxygen octahedra) in the tetragonal phase (where it belongs to the A_1 mode) came out in much better agreement with experiment in our previous calculations of Ref. [9]. For the A_2 phonon, the difference seems to be due to anharmonicity effects as has been already supposed in Ref. [9]. The explicit form of the total energy fit for this mode, which we found to be ΔE (mRy) = $15.16 (S_5)^2 + 12.99 (S_5)^4$ (S_5 in a.u.), makes it possible to calculate the relevant frequency beyond the harmonic approximation, that is done in Section IV.

IV. QUANTUM OSCILLATOR TREATMENT

Since the total energy as function of symmetrized displacements was available from our calculations in a sufficient number of points for providing the fourth-order polynomial fit, an extension of our analysis beyond the harmonic

approximation becomes feasible. Rather than introducing anharmonic corrections to frequencies obtained in the previous section, we preferred to solve the Schrödinger equation for an, in principle, multidimensional quantum oscillator with a general-shape potential. We solved the Schrödinger equation numerically, by a finite-difference method (see, e.g., Ref. [18,19]), so that no basis functions have been employed.

Similarly to how it was described elsewhere for the classical harmonic oscillator [15], we use an arbitrary convenient set of symmetry-adapted displacement coordinates $S_t = \sum_i B_{ti} x_i$ (x_i are conventional cartesian displacements), which form a complete basis within a particular irreducible representation, but do not need to be orthonormal. Then, the Schrödinger equation acquires a form:

$$\left[-\frac{\hbar^2}{2} \sum_{tt'} \frac{\partial}{\partial S_t} G_{tt'} \frac{\partial}{\partial S_{t'}} + V(\{S_t\}) \right] \Psi = E \Psi$$

where $G_{tt'} = \sum_i B_{ti} m_i^{-1} B_{t'i}$ is the kinetic-energy matrix. Mixed derivatives can further be excluded (that is desirable for maintaining high sparseness of the finite-difference matrix) by the following orthogonalizing transformation:

$$Q_t = \sum_{t'} \frac{X_{t't}}{\sqrt{\lambda^t}} S_{t'},$$

where $X_{t't}$ is the t -th eigenvector, corresponding to the eigenvalue λ^t , of the kinetic energy matrix.

The energy differences between the zero-point energy level and subsequent higher states give rise to characteristic frequencies of several lowest phonon modes. For the total energy fitted by the second order polynomial, these lowest frequencies should exactly coincide with the classical frequencies obtained in the harmonic approximation. This provides an additional mean of testing the accuracy of the finite-difference calculation scheme. Apart from allowing the anharmonicity in the most general way, the quantum treatment provides the description of high-frequency phonon branches (i.e. those lying beyond the lower $3N - 6$ optical modes) and paves a way to incorporating the temperature effects. The energy levels of the oscillator may be further populated according to the Bose–Einstein statistics, and the transitions between levels analyzed. An analysis of this kind has been done by Bakker *et al.* [20] for a one-dimension quantum oscillator model of the A_1 phonon in LiTaO₃.

The accuracy of the calculation is essentially limited by the finiteness of the discrete mesh, and the convergence of eigenvalues in this parameter was explicitly controlled; however for the 4-dimensional oscillator (A_1 and B_2 irreducible representations), the maximal manageable grid of $14^4=38416$ points was not sufficiently dense to produce as stable frequencies as those for B_1 and A_2 modes.

For the B_2 mode, the lowest energy levels of the 3-dimensional quantum oscillator were found to be 64, 89, and 130 cm^{-1} . Thus, the lowest possible phonon frequency is 25 cm^{-1} , that is of correct order of magnitude, as compared with the experimental soft mode frequency (the harmonic approximation could only provide an information that the corresponding mode is indeed soft). Because of the small energy differences between several lowest oscillator levels, corresponding transitions can be easily excited already at medium temperatures, thus leading to a substantial increase of the soft mode frequency on heating. We however did not consider this effect in detail.

For the one-dimensional A_2 problem, the five lowest energy levels of the quantum oscillator are: 116, 357, 612, 880 and 1160 cm^{-1} . The lowest transition energy is therefore 241 cm^{-1} that is already an improvement over the result obtained in the harmonic approximation. The gradual increase of the separation between subsequent higher levels would result in somehow higher mean frequencies at elevated temperatures, but this effect is expected to be much smaller than for the soft mode.

V. ATOMIC DISPLACEMENTS WITHIN THE SOFT MODE

Now that the whole total energy hypersurface is mapped as function of symmetrized displacements of atoms from their equilibrium positions in the orthorhombic structure, it becomes possible to analyze the finite distortion compatible with the soft B_2 mode which is a precursor of the orthorhombic to rhombohedral phase transition. We did not consider the change in the lattice strain which is an important element of such transition. Nevertheless, it makes some sense to compare the symmetry-lowering displacements of atoms from equilibrium positions in the orthorhombic phase with the experimental geometry of the rhombohedral phase.

We performed some additional fine-mesh fit near the position of the total energy minimum, in order to determine the x -displacements of atoms with better accuracy than it is possible from the global fit by the 4th order polynomial. The equilibrium displacements of K, Nb and O(I) in the [100] direction from the positions listed in Table I are 0.006 Å, -0.043 Å and 0.013 Å, correspondingly; they result in the total energy lowering of 0.06 mRy per formula unit.

An additional degree of freedom enabling the displacement of Nb in the \mathbf{z} direction along with that in \mathbf{x} (i.e. the relaxation within both B_2 and A_1 modes) did not result in any better total energy minimum. The relative positions of thus displaced atoms projected on the (\mathbf{x}, \mathbf{z}) plane of the orthorhombic cell are shown in Fig. 1 in comparison with the experimentally determined positions in the rhombohedral phase.

Magnitudes of the \mathbf{x} -displacements of Nb and O in the rhombohedral phase are somehow larger than within the "frozen" soft mode. Otherwise, the most pronounced difference is the underestimated \mathbf{z} -displacement of K, as has been already mentioned in section II.

It is of considerable interest to know whether the displacements compatible with the B_2 symmetry are energetically favourable if they occur only globally, simultaneously over the crystal, or also locally, on a short-range scale, as may be expected from the eight-site model (see, e.g., Ref. [6] for the discussion on the latter). We addressed this problem early for the case of tetragonal soft-mode displacements from the cubic phase [21], and it was established that the [001] displacements result in a total energy lowering when they occur simultaneously in all unit cells, but not if they occur only in 25% of cells, as was tested in a supercell calculation. In other words, it is the indication that the cubic to tetragonal ferroelectric transition cannot be triggered by a spontaneous displacement of a single Nb atom, but rather needs a larger self-supporting region where such transformation occurs. [22] Unfortunately, we could not give any estimates as for the size or shape of such regions from our supercell calculations. With respect to the orthorhombic phase of KNbO_3 , the similar theoretical study of the effect of local displacements was motivated by recent experimental observation by Dougherty *et al.* [7] of relaxation processes in time-resolved Raman spectra which have been attributed to the hoppings, compatible with the A_1 mode, over three classes of off-center Nb sites, distinguished by symmetry. There was however no experimental information available as for the spatial extent of spatial correlations in such relaxation processes.

We tried to analyze several patterns of local displacements in the orthorhombic phase in supercell calculations, in order to establish some most important trends. Since it was not feasible to optimize the geometry in a supercell calculation in terms of all relevant atomic displacements, we limited ourselves to the study of the effect of pure Nb displacements which are obviously dominant. The incorporation of the relaxation of other atoms may somehow correct the magnitudes of the energy differences, but hardly the underlying qualitative trends. We considered local Nb displacements along \mathbf{z} and \mathbf{x} , i.e. those compatible with A_1 and B_2 modes, from the equilibrium position defined in Table I. The relevant crystal superstructures modelled by $2 \times \text{KNbO}_3$ and $4 \times \text{KNbO}_3$ supercells are schematically shown in Figures 2 and 3, along with corresponding total energy dependencies.

Fig. 2 shows the effect on the total energy of \mathbf{z} -displacements of every fourth "impurity" Nb atom, while other three Nb's in the supercell are kept fixed and provide a bulk macroscopic polarization. Apart from the minimum corresponding to $\Delta_z(\text{Nb})=0.$, the total energy grows rapidly; the displacement against the electrostatic field (A_1 mode) through the centre of the O_6 nearest-neighbor octahedra to the symmetric position increases the total energy by about 30 mRy. Compared to the tiny value of 0.06 mRy energy lowering due to subsequent \mathbf{x} -displacement (B_2 mode) into one of "eight sites" nearest to this point, it leaves no chance to find there a local minimum of the total energy with respect to both Δ_z and Δ_x variables. The contradiction with the experimental evidence of Ref. [7] that there *are* relaxation-type hoppings of the A_1 symmetry between distinct local minima is apparently resolved by realizing that in the experiment, a considerable number of neighboring Nb atoms undergoes a relaxation hopping simultaneously, depending on the energy pumped in. A limiting case where really *all* atoms in crystal are involved in this process would mean the inversion of polarization, correspondingly mapping the total energy minima into new positions through the center of the unit cell.

Another choice of $4 \times \text{KNbO}_3$ supercell where "impurity" Nb atoms are organized in chains along the \mathbf{z} direction (Fig. 2b) leads to the same type of the energy dependence versus the displacement magnitude. It indicates that the local displacements against the bulk polarization are the main energetically unfavourable factors, whereas local frustrations within the \mathbf{z} -chains of interchanging "impurity" and "bulk" atoms, which are peculiar for the first supercell geometry, are of minor importance.

In contrary to this type of behavior, the \mathbf{x} -displacements normal to the direction of macroscopic polarisation (B_2 mode) were found to be energetically favourable even if not supported by a similar displacement of near neighbors. This is in itself a clear indication of the order-disorder phase transition type from orthorhombic to rhombohedral structure. The precise energetics for different patterns of "up"- and "down"- Nb displacements from the (\mathbf{y}, \mathbf{z}) plane deserves however more detailed investigation. In addition to the perfect phase with the "frozen out" B_2 phonon (Fig. 3a), we considered two types of $2 \times \text{KNbO}_3$ supercells which combine "up" and "down" displacements in two different ways: a chessboard arrangement with chains of identically shifted Nb atoms in the \mathbf{x} direction (Fig. 3b) and a NaCl-type structure where such chains are broken (Fig. 3c). The corresponding total energy differences show that the last structure with frustrations in the \mathbf{x} direction due to broken chains is absolutely unstable. Among two other structures which both contain undistorted chains, the one where "up" and "down"-chains appear in mixture is definitely more stable. An important consequence from this fact is its full agreement with the "chain structure" of the orthorhombic phase as proposed by Comes *et al.* [23], whereas any other mixture of "up"- and "down" displacements

which incorporates frustrations in the \mathbf{x} direction can be relatively safely discarded. Another important consequence regards the mutual arrangement of chains. There seems to be a certain correlation within the (\mathbf{y}, \mathbf{z}) plane which favours each chain to have the neighboring chains with the opposite direction of displacement. In order to check that this statement is not confined to the particular chessboard geometry of the supercell in Fig. 3b, we performed an additional calculation where the effect of the displacement reversal within one chain out of four in the initial "perfect" geometry of Fig. 3a has been studied. This was our possibly best supercell approximation to the displacement reversal within just one single chain in crystal at all, because thus reversed chains do not contact in this geometry. The result is that the spontaneous, say, "down" reversal of Nb displacements within one chain, with respect to the uniform background of "up" displacements, lowers the total energy by ~ 0.01 mRy per formula unit, i.e. *is* energetically favourable. The interaction between chains then works until some particular pattern with equal number of "up" and "down" chains is established. This stabilizes the orthorhombic structure, unless the lattice strain is allowed to become an independent parameter, and the system finds another global energy minimum compatible with the rhombohedral space group.

Since the energy lowering due to \mathbf{x} -displacements is smaller than the zero-point energy of the quantum oscillator in a potential well related to the B_2 mode vibrations, it is worth noting that the above mentioned finite "up" and "down" displacements should not be understood literally, like well defined "frozen" atomic positions at zero temperature. Rather, we have to do with a damped quantum solution (in agreement with experimental observation of heavily damped B_2 modes, Ref. [7]) which is symmetric with respect to "up" and "down" \mathbf{x} -directions for each single quantum oscillator. The interaction between chains distorts the symmetry of each individual solution due to the coupling between oscillators, and the mean value of corresponding \mathbf{x} -displacement gets accordingly displaced. Its average over the whole system however remains zero.

VI. SUMMARY

We extended our previous theoretical study of TO Γ phonons in KNbO_3 to the orthorhombic phase. Based on the total energy calculations and polynomial fit of the results versus atomic displacements compatible with different irreducible representations, classical frozen phonon frequencies and corresponding eigenvectors have been calculated in the harmonic approximation, in satisfactory agreement with experimental data. For A_2 and B_2 modes, the quantum oscillator analysis has been done as well, resulting in some corrections to classical harmonic frequencies. The microscopic structure of the orthorhombic phase has been further analyzed in a series of supercell calculations modelling several patterns of Nb [100]-displacements compatible with the B_2 mode. It was established that the formation of chains of uniformly displaced Nb atoms along the [100] direction is highly energetically favourable, in agreement with the experimental observations of the chain structure. The interaction between chains then favours the zero value of the average [100] Nb displacement, stabilizing the orthorhombic structure.

ACKNOWLEDGMENTS

The authors are grateful to M. Methfessel for his assistance and advise in using his full-potential LMTO code, and to T. Dougherty and H. Bakker for providing manuscripts of their papers prior to publication and for stimulating discussions. Consultations with by M. Shamonin and P. Hertel were essential for getting acquaintance of practical finite-difference schemes. Financial support of the Deutsche Forschungsgemeinschaft (SFB 225, Graduate College) is gratefully acknowledged.

* On leave from Institute of Metal Physics, Russian Academy of Sciences, Yekaterinburg, Russia. Electronic address: apostnik@physik.uni-osnabrueck.de

- [1] D. G. Boziniš and J. P. Hurrell, *Phys. Rev. B* **13**, 3109 (1976).
- [2] A. M. Quittet, M. I. Bell, M. Krauzman, and P. M. Raccach, *Phys. Rev. B* **14**, 5068 (1976).
- [3] M. D. Fontana, A. Ridah, G. E. Kugel, and C. Carabatos-Nedelec, *J. Phys. C* **21**, 5853 (1988).
- [4] R. Currat, R. Comès, B. Dorner, and E. Wiesendanger, *J. Phys. C: Solid State Phys.* **7**, 2521 (1974).
- [5] N. de Mathan, E. Prouzet, E. Husson, and H. Dexpert, *J. Phys.: Condens. Matter* **5**, 1261 (1993).
- [6] T. P. Dougherty, G. P. Wiederrecht, K. A. Nelson, M. H. Garret, H. P. Jensen, and C. Warde, *Science* **258**, 770 (1992).

- [7] T. P. Dougherty, G. P. Wiederrecht, and K. A. Nelson, to be published in Phys. Rev. B (1994); T. P. Dougherty, G. P. Wiederrecht, and K. A. Nelson, to be published in Ferroelectrics (1994).
- [8] A. V. Postnikov, T. Neumann, G. Borstel, and M. Methfessel, Phys. Rev. B **48**, 5910 (1993).
- [9] A. V. Postnikov, T. Neumann, and G. Borstel, Phys. Rev. B **51**, (1994).
- [10] M. Methfessel, Phys. Rev. B **38**, 1537 (1988).
- [11] M. Methfessel, C. O. Rodriguez, and O. K. Andersen, Phys. Rev. B **40**, 2009 (1989).
- [12] M. Methfessel, M. van Schilfhaarde, Phys. Rev. B **48**, 4937 (1993).
- [13] Of course the accuracy of 0.01 mRy applies only to the trends in the total energy calculated for different geometries but with otherwise identical setup, and not to the absolute total energy values which are sensitive, e.g., to the choice of muffin-tin sphere radii within much broader limits.
- [14] A. W. Hewat, J. Phys. C **6**, 2559 (1973).
- [15] R. E. Cohen and H. Krakauer, Phys. Rev. B **42**, 6416 (1990).
- [16] E. B. Wilson, Jr., J. C. Decius, and P. C. Cross, *Molecular Vibrations: The Theory of Infrared and Raman Vibrational Spectra* (McGraw-Hill, New York, 1955).
- [17] M. D. Fontana, G. Métrat, J. L. Servoin, and F. Gervais, J. Phys. C **17**, 483 (1984).
- [18] A. R. Mitchell and D. F. Griffiths, *The Finite Difference Method in Partial Differential Equations* (John Wiley, Chichester, 1980).
- [19] W. F. Ames, *Numerical Methods for Partial Differential Equations* (Academic Press, New York, 1977).
- [20] H. J. Bakker, S. Hunsche, and H. Kurz, Phys. Rev. B **48**, 9331 (1993).
- [21] A. V. Postnikov, T. Neumann, and G. Borstel, to be published in Ferroelectrics (1994).
- [22] This is not in contradiction with the eight-site model the essential statement of which is that Nb atoms occupy off-center [111]-type displaced positions in all crystallographic phases of KNbO₃. Our calculation result just cited indicates that hoppings over such displaced positions do not occur independently in adjacent unit cells, but rather exhibit some spatial coherence.
- [23] R. Comes, M. Lambert, and A. Guinier, Solid State Commun. **6**, 715 (1968).

FIG. 1. Displacements of atoms, relative to the center of mass, in the (\mathbf{x}, \mathbf{z}) plane of orthorhombic KNbO₃: from geometry optimization based on total energy calculations (black circles); from neutron diffraction measurements in the rhombohedral phase, Ref. [14] (open circles).

FIG. 2. Total energy differences (per formula unit) versus \mathbf{z} -displacements of Nb from the equilibrium position for two superstructures. Thick line contours the supercell used.

FIG. 3. Total energy differences (per formula unit) versus \mathbf{x} -displacements of Nb from nominally equilibrium position in the orthorhombic structure for three superstructures. Thick line contours the supercell used.

TABLE I. Positions of atoms in orthorhombic phase of KNbO₃ (in terms of lattice parameters) as determined by neutron diffraction measurements, Ref. [14], and optimized in the FP-LMTO total-energy calculation.

	Atom	a	b	c		Δ_{exp}	Δ_{calc}
1	K	0	0	Δ_z		0.0138	0.0367
2	Nb	$\frac{1}{2}$	0	$\frac{1}{2}$			
3	O(I)	0	0	$\frac{1}{2} + \Delta_z$	}	0.0364	0.0326
4	O(II)	$\frac{1}{2}$	$\frac{1}{4} + \Delta_y$	$\frac{1}{4} + \Delta_z$			
5	O(II)	$\frac{1}{2}$	$\frac{3}{4} - \Delta_y$	$\frac{1}{4} + \Delta_z$			
					$\Delta_z :$	0.0342	0.0323
					$\Delta_y :$	-0.0024	-0.0062

TABLE II. Symmetry coordinates used in the phonon calculations for four irreducible representations of orthorhombic KNbO₃.

A_1	A_2	B_1	B_2
$S_1 = Z_1 - \frac{1}{2}(Z_4 + Z_5)$	$S_5 = X_4 - X_5$	$S_6 = Y_1 - \frac{1}{2}(Y_4 + Y_5)$	$S_{10} = X_1 - \frac{1}{2}(X_4 + X_5)$
$S_2 = Z_2 - \frac{1}{2}(Z_4 + Z_5)$		$S_7 = Y_2 - \frac{1}{2}(Y_4 + Y_5)$	$S_{11} = X_2 - \frac{1}{2}(X_4 + X_5)$
$S_3 = Z_3 - \frac{1}{2}(Z_4 + Z_5)$		$S_8 = Y_3 - \frac{1}{2}(Y_4 + Y_5)$	$S_{12} = X_3 - \frac{1}{2}(X_4 + X_5)$
$S_4 = Y_4 - Y_5$		$S_9 = Z_4 - Z_5$	

TABLE III. 4th order polynomial fit of the total energy (in mRy) in terms of the symmetry coordinates of the B_2 representation (in a.u.).

powers of			Coef.	powers of			Coef.	powers of			Coef.
S_{10}	S_{11}	S_{12}		S_{10}	S_{11}	S_{12}		S_{10}	S_{11}	S_{12}	
2	0	0	30.70	3	1	0	-7.02	1	1	2	-1316.91
1	1	0	-2.84	3	0	1	-300.44	1	0	3	-876.50
1	0	1	-61.27	2	2	0	-57.52	0	4	0	414.92
0	2	0	-2.76	2	1	1	1160.64	0	3	1	-1359.44
0	1	1	57.91	2	0	2	847.09	0	2	2	1549.71
0	0	2	83.73	1	3	0	41.03	0	1	3	-925.13
4	0	0	84.82	1	2	1	386.80	0	0	4	214.28

TABLE IV. Calculated Γ -TO frequencies and eigenvectors in orthorhombic KNbO_3 .

Symm.	Frequency (cm^{-1})	Polarization	Eigenvectors				
			K	Nb	O_1	O_2	O_3
A_1	186	$\begin{cases} y \\ z \end{cases}$	-0.86	0.48	-0.03	0.07	-0.07
	257	$\begin{cases} y \\ z \end{cases}$	0.15	-0.00	-0.77	0.10	0.10
	307	$\begin{cases} y \\ z \end{cases}$	-0.14	-0.48	-0.77	0.34	-0.34
	593	$\begin{cases} y \\ z \end{cases}$	0.08	0.15	0.50	0.28	0.28
A_2	224	x				0.25	-0.25
B_1	146	$\begin{cases} y \\ z \end{cases}$	-0.85	0.50	0.00	0.57	-0.57
	232	$\begin{cases} y \\ z \end{cases}$	0.07	-0.09	-0.63	0.07	0.07
	297	$\begin{cases} y \\ z \end{cases}$	-0.19	-0.46	0.67	0.08	-0.08
	528	$\begin{cases} y \\ z \end{cases}$	0.13	0.12	0.26	0.39	-0.39
		$\begin{cases} y \\ z \end{cases}$				0.36	0.36
B_2	82i	x	0.48	-0.69	0.43	0.16	-0.16
	185	x	-0.73	0.01	0.32	-0.37	-0.37
	467	x	0.13	-0.10	-0.79	0.56	-0.56

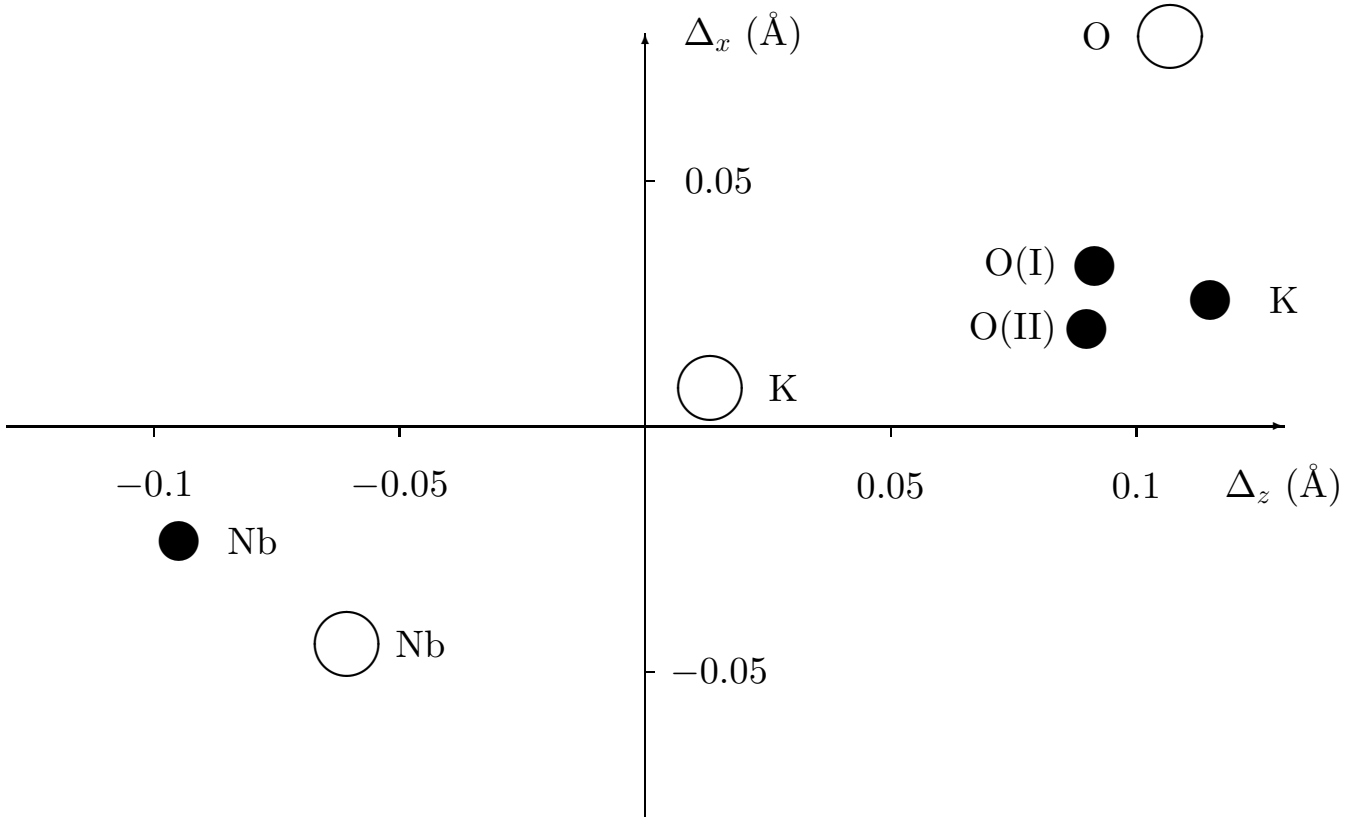
TABLE V. Calculated and measured frequencies of Γ -TO phonons in orthorhombic KNbO_3 .

Mode	Symm.	Calculated frequency (cm^{-1})	Expt. ^a	Expt. ^b	Expt. ^c
TO ₁	B_2	soft	56	40	59
	B_1	232	243	249	
	A_1	257	290	281.5	
TO ₂	B_2	185	195	196.5	197.5
	B_1	146	187	192	
	A_1	186	190	193	
TO ₃	B_2	467	511	513	516
	B_1	528	534	534	
	A_1	593	607	606.5	
TO ₄	B_1	297	270	270	
	A_1	307	299	297	
	A_2	224	283	283	

^aRaman spectroscopy; Ref. [1].

^bRaman spectroscopy; Ref. [2].

^cInfrared spectroscopy; Ref. [17].



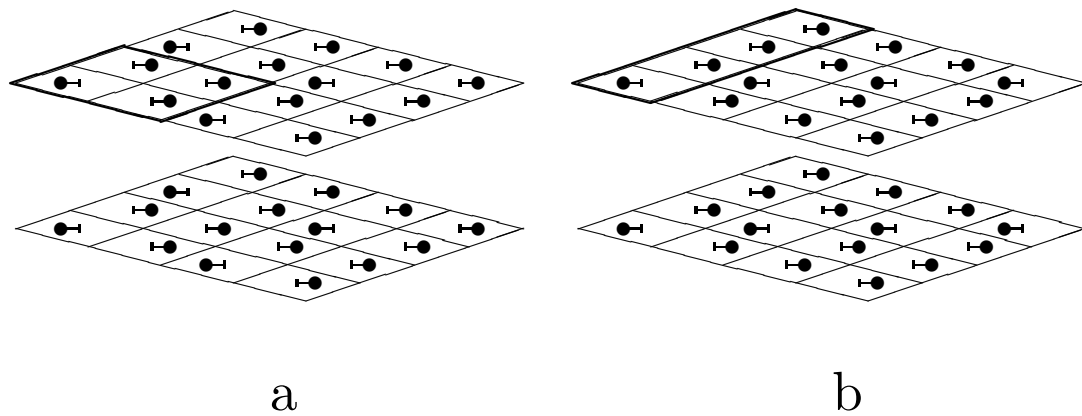
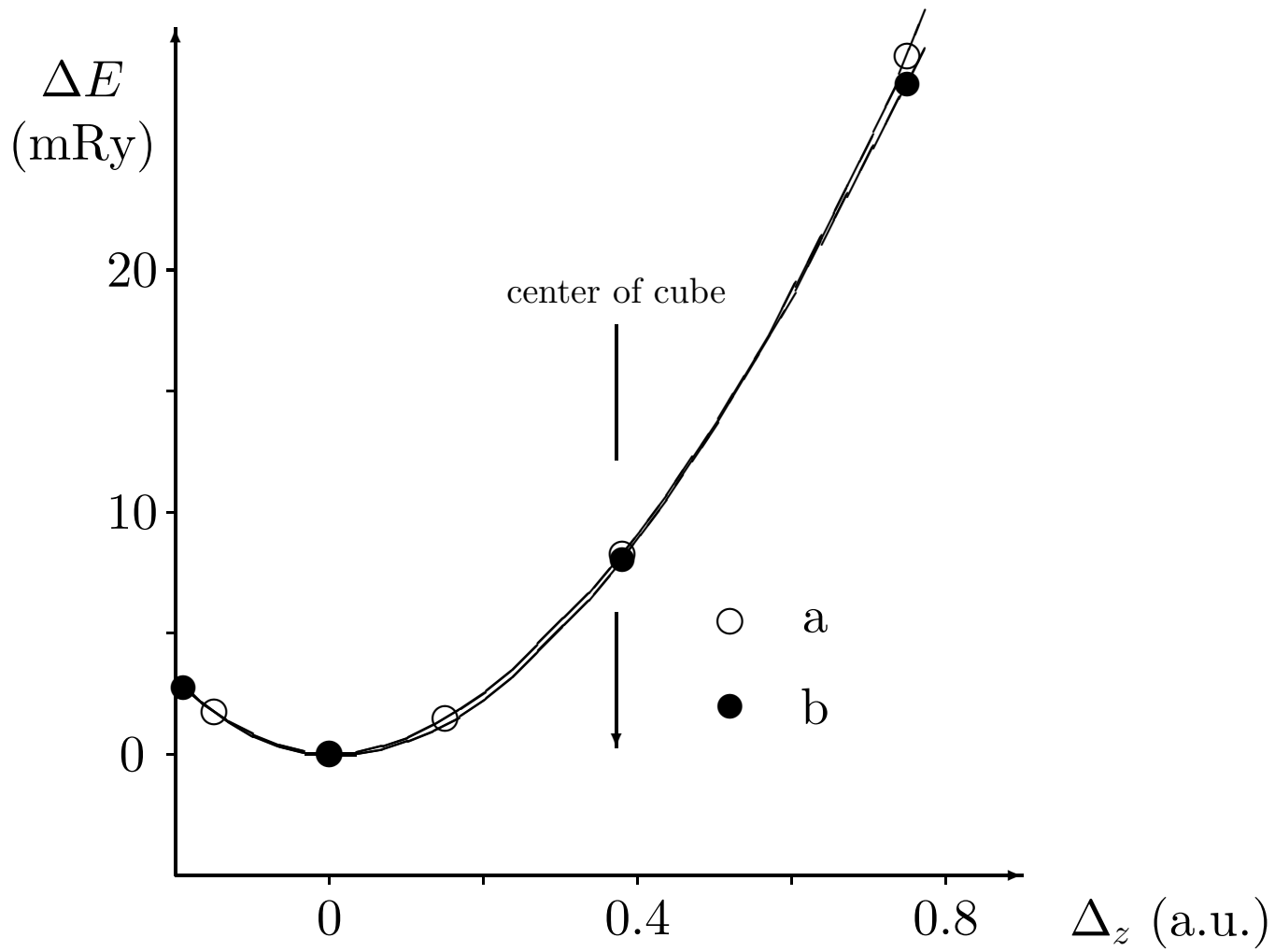


Fig. 2

ΔE
(mRy)

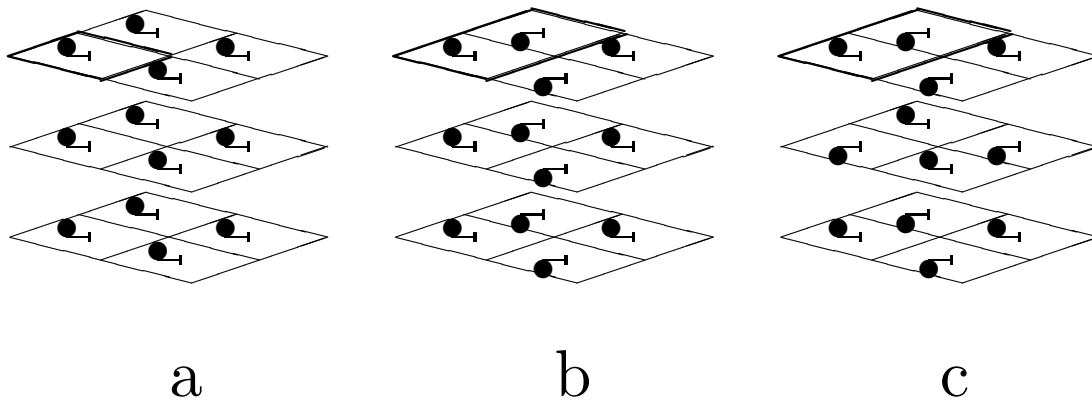
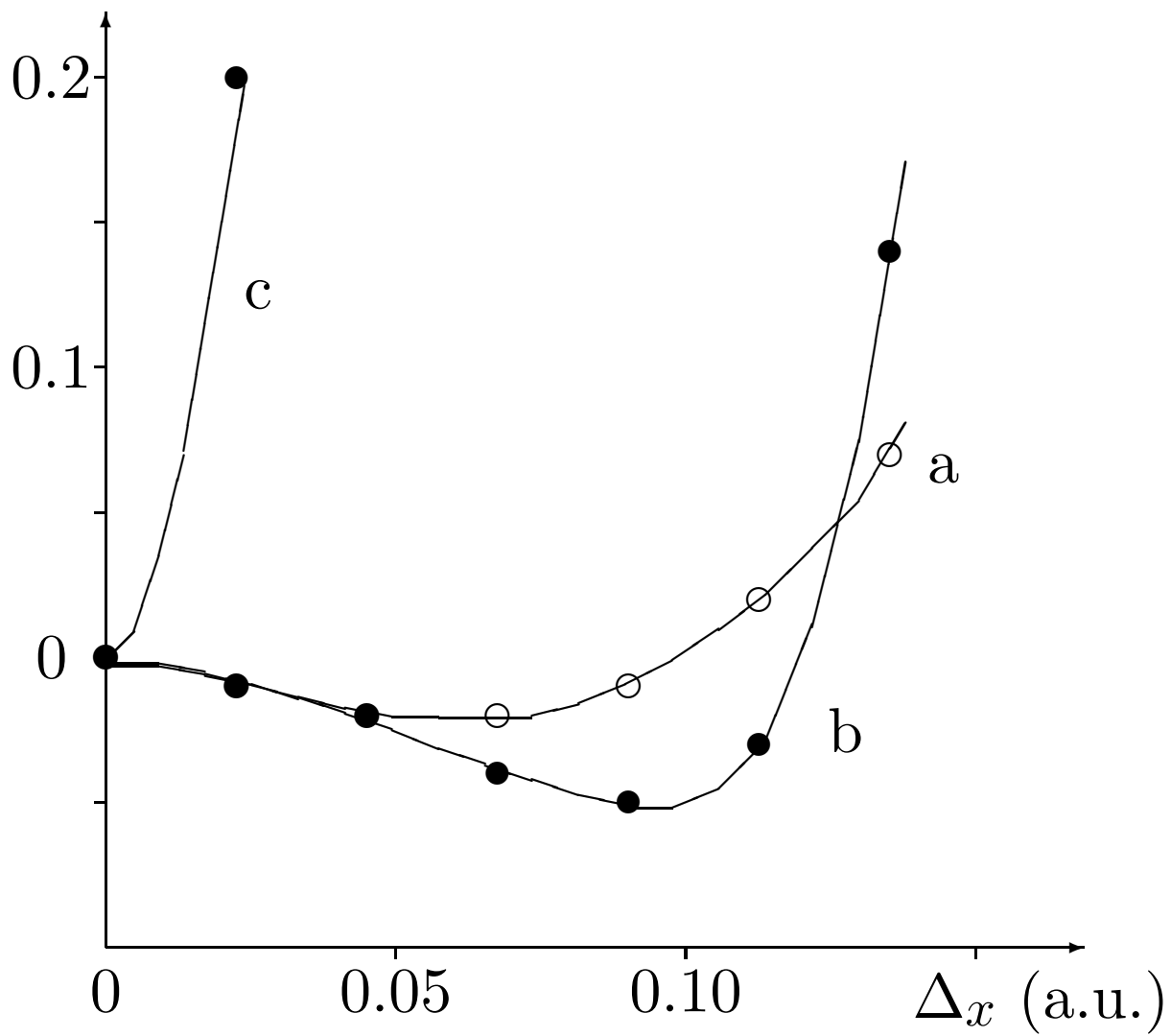


Fig. 3